Inorg. Chem. **2006**, *45*, 5510–5520

Model Peptides Based on the Binding Loop of the Copper Metallochaperone Atx1: Selectivity of the Consensus Sequence MxCxxC for Metal Ions Hg(II), Cu(I), Cd(II), Pb(II), and Zn(II)

Pierre Rousselot-Pailley,[†] Olivier Sénèque,[†,‡] Colette Lebrun,[†] Serge Crouzy,[§] Didier Boturyn,[||] Pascal Dumy,[||] Michel Ferrand,[§] and Pascale Delangle*[,†]

Laboratoire de Reconnaissance Ionique, DRFMC/LCIB (UMR_E 3 CEA-UJF), CEA-Grenoble, 17 rue des Martyrs, F-38054 Grenoble Cedex 9, France, Laboratoire de Biophysique Moléculaire et Cellulaire (UMR 5090), DRDC, CEA-Grenoble, 17 rue des Martyrs, F-38054 Grenoble Cedex 9, France, and, Université Joseph Fourier, 301 rue de la Chimie, 38041 Grenoble Cedex 9, France

Received March 14, 2006

The amino acid sequence MxCxxC is conserved in many soft-metal transporters that are involved in the control of the intracellular concentration of ions such as Cu(I), Hg(II), Zn(II), Cd(II), and Pb(II). A relevant task is thus the selectivity of the motif MxCxxC for these different metal ions. To analyze the coordination properties and the selectivity of this consensus sequence, we have designed two model peptides that mimic the binding loop of the copper chaperone Atx1: the cyclic peptide P^C c(GMTCSGCSRP) and its linear analogue P^L (Ac-MTCSGCSRPG-NH_2). By using complementary analytical and spectroscopic methods, we have demonstrated that 1:1 complexes are obtained with Cu(I) and Hg(II), whereas 1:1 and 1:2 (M:P) species are successively formed with Zn(II), Cd(II), and Pb(II). The complexation properties of the cyclic and linear peptides are very close, but the cyclic compound provides systematically higher affinity constants than its unstructured analogue. The introduction of a xPGx motif that forms a type II β turn in P^C induces a preorganization of the binding loop of the peptide that enhances the stabilities of the complexes (up to 2 orders of magnitude difference for the Hg complexes). The affinity constants were measured in the absence of any reducing agent that would compete with the peptides and range in the order Hg(II) > Cu(I) $\gg$ Cd(II) > Pb(II) > Zn(II). This sequence is thus highly selective for Cu(I) compared to the essential ion Zn(II) that could compete in vivo or compared to the toxic ions Cd(II) and Pb(II). Only Hg(II) may be an efficient competitor of Cu(I) for binding to the MxCxxC motif in metalloproteins.

Introduction

Metallic elements play major roles in biochemistry; the essential transition-metal ions are accumulated by cells that employ them in structurally constrained binding sites in metalloproteins, where they can carry out structural, regulatory, or catalytic roles. Because these metal ions can also catalyze cytotoxic reactions, several families of proteins are present in the cells to control their concentration and to confine them to vital roles.[1−3] Proteins involved in the protection and delivery of metal ions to their targets include membrane transporters such as ATP-driven heavy-metal pumps,[4] metalloregulatory sensors,[3] and cytoplasmic proteins.[5,6]

* To whom correspondence should be addressed. E-mail: pascale.delangle@cea.fr. Tel: (+33) 4 38 78 98 22. Fax: (+33) 4 38 78 50 90.

[†] Laboratoire de Reconnaissance Ionique, DRFMC/LCIB (UMR_E 3 CEA-UJF), CEA-Grenoble.

[‡] Present address: Laboratoire de Physicochimie des Métaux en Biologie (UMR 5155 CEA-CNRS−UJF), DRDC, CEA-Grenoble, 17 rue des Martyrs, 38054 Grenoble Cedex 9, France.

[§] Laboratoire de Biophysique Moléculaire et Cellulaire (UMR 5090), DRDC, CEA-Grenoble.

[||] Laboratoire d'Etudes Dynamiques et Structurales de la Sélectivité (UMR 5616).

(1) Holm, R. H.; Kennepohl, P.; Solomon, E. I. *Chem. Rev.* **1996**, *96*, 2239−2314.
(2) Finney, L. A.; O'Halloran, T. V. *Science* **2003**, *300*, 931−936.
(3) Tottey, S.; Harvie, D. R.; Robinson, N. J. *Acc. Chem. Res.* **2005**, *38*, 775−783.
(4) Solioz, M.; Vulpe, C. *Trends Biochem. Sci.* **1996**, *21*, 237−241.
(5) Rosenzweig, A. C. *Acc. Chem. Res.* **2001**, *34*, 119−128.
(6) O'Halloran, T. V.; Culotta, V. C. *J. Biol. Chem.* **2000**, *275*, 25057−25060.

10.1021/ic060430b CCC: $33.50
Published on Web 06/08/2006

Among these metals, Cu is an essential element that is used as a cofactor in many redox proteins, involved in several vital processes. Because free Cu can promote Fenton-like reactions and thus would be very toxic even at low concentration, the intracellular Cu concentration needs to be rigorously controlled so that Cu is only provided to the essential enzymes but does not accumulate to toxic levels.[5,7] The intracellular Cu-trafficking systems in yeast are among the best understood.[8] Soluble cytosolic proteins, namely, metallochaperones, deliver Cu to specific target proteins. The Cu delivery pathways start with metal importation by the Ctr membrane transporters.[9] Once inside the cytosol, the chaperone Atx1 shuttles Cu to an intracellular Cu transporter (Ccc2) located in the Golgi compartment of the secretory pathway. Then Ccc2 pumps the metal into the lumen of the Golgi for insertion into Cu enzymes.[10] Homologues of Atx1 have been identified in humans (Hah1), bacteria, plants, and animals.[11,12]

Atx1 is a 73 amino acid protein that binds Cu in the 1+ oxidation state.[13,14] Copper ATPases such as Ccc2 in yeast and its human homologues, the Menkes (MNK)[15−17] and Wilson (WND)[18,19] proteins, possess a variable number of N-terminal Atx1-like cytoplasmic domains.[5,7,20] Atx1 and these soluble metal binding domains (MBDs) share a classical "ferredoxin-like" $\beta\alpha\beta\beta\alpha\beta$ fold in which four β strands and two α helices are connected by loop regions and contain a conserved N-terminal MxCxxC sequence motif that binds metal ions with two cysteines.[21−26]

The MxCxxC motif is also conserved in many soft-metal transporters such as merP, a soluble Hg-transport protein,[27] or ZntA, a Zn-trafficking P-type ATPase, which binds Zn(II) via an aspartate O atom in addition to the two cysteine S atoms.[28] The transporter ZntA is also a Pb(II)/Cd(II) export protein.[29,30] The MxCxxC consensus sequence has been demonstrated to bind several soft-metal ions, like Hg(II), Cu(I), Zn(II), Pb(II), and Cd(II).[31,32] Nevertheless, the factors that govern the selectivity of these metal transporters in vivo remain unclear.[3] An important task is thus the selectivity of this sequence for the different metal ions cited above.

The design of chemical models of these proteic MBDs is helpful to approach in vitro the metal/ligand interactions and can thus lead to a better understanding of the complexation properties of these metalloproteins. Moreover, they can lead to the conception of new selective complexing agents derived from Atx1-like transporters for the decorporation, depollution, or design of biosensors. The most intuitive design approach in building models of this binding loop is to study peptides based on the protein binding site. This approach was evidenced to be valuable for modeling the structure and the function of metalloproteins for metal ions such as Pb(II), Hg(II), Cd(II), and Cu(I).[31,33−38] Therefore, we chose to use synthetic peptides to test the selectivity of the binding sequences found in metal-trafficking proteins, to better understand the selectivity of these sequences for heavy-metal ions bound in vivo.

We have recently described the design of the cyclic peptide P^C chosen to mimic the binding loop of the chaperone Atx1.[39] This model compound described in Figure 1 provides (i) the binding sequence MTCSGCS of the copper chaperone, (ii) a charged amino acid (R) to mimic the proximal Lys65 side chain standing next to the metal binding site of Atx1 and to increase the solubility in water, and (iii) a xPGx motif able to form a β turn, which rigidifies the cyclopeptide and acts as an anchor for the metal binding site. We have demonstrated that this peptide was able to bind a series of metal

(7) Arnesano, F.; Banci, L.; Bertini, I.; Ciofi-Baffoni, S. *Eur. J. Inorg. Chem.* **2004**, 1583−1593.
(8) Puig, S.; Thiele, D. J. *Curr. Opin. Chem. Biol.* **2002**, *6*, 171−180.
(9) Dancis, A.; Yuan, D. S.; Haile, D.; Askwith, C.; Eide, D.; Moehle, C.; Kaplan, J.; Klausner, R. D. *Cell* **1994**, *76*, 393−402.
(10) Huffman, D. L.; O'Halloran, T. V. *J. Biol. Chem.* **2000**, *275*, 18611−18614.
(11) Klomp, L. W. J.; Lin, S.-J.; Yuan, D. S.; Klausner, R. D.; Cullota, V. C.; Gitlin, J. D. *J. Biol. Chem.* **1997**, *272*, 9221−9226.
(12) Hung, I. H.; Casareno, R. L. B.; Labesse, G.; Mathews, F. S.; Gitlin, J. D. *J. Biol. Chem.* **1998**, *273*, 1749−1754.
(13) Pufahl, R. A.; Singer, C. P.; Peariso, K. L.; Lin, S.-J.; Schmidt, P. J.; Fahrni, C. J.; Culotta, V. C.; Penner-Hahn, J. E.; O'Halloran, T. V. *Science* **1997**, *278*, 853−856.
(14) Arnesano, F.; Banci, L.; Bertini, I.; Huffman, D. L.; O'Halloran, T. V. *Biochemistry* **2001**, *40*, 1528−1539.
(15) Vulpe, C.; Levinson, B.; Whitney, S.; Packman, S.; Gitschier, J. *Nat. Gen.* **1993**, *3*, 7−13.
(16) Chelly, J.; Tümer, Z.; Tonnesen, T.; Petterson, A.; Ishikawa-Brush, Y.; Tommerup, N.; Horn, N.; Monaco, A. P. *Nat. Gen.* **1993**, *3*, 14−19.
(17) Mercer, J. F. B.; Livingston, J.; Hall, B.; Paynter, J. A.; Begy, C.; Chandrasekharappa, S.; Lokhart, P.; Grimes, A.; Bhave, M.; Siemieniak, D.; Glover, T. W. *Nat. Gen.* **1993**, *3*, 20−25.
(18) Bull, P. C.; Thomas, G. R.; Rommens, J. M.; Forbes, J. R.; Cox, D. W. *Nat. Gen.* **1993**, *5*, 327−337.
(19) Tanzi, R. E.; Petrukhin, K.; Chernov, I.; Pellequer, J. L.; Wasco, W.; Ross, B.; Romano, D. M.; Parano, E.; Pavone, L.; Brzustowicz, L. M.; Devoto, M.; Peppercorn, J.; Bush, A. I.; Sternlieb, I.; Pirastu, M.; Gusella, J. F.; Evgrafov, O.; Penchaszadeh, G. K.; Honig, B.; Edelman, I. S.; Soares, M. B.; Scheinberg, I. H.; Gilliam, T. C. *Nat. Gen.* **1993**, *5*, 344−350.
(20) Arnesano, F.; Banci, L.; Bertini, I.; Ciofo-Baffoni, S.; Molteni, E.; Huffman, D. L.; O'Halloran, T. V. *Genome Res.* **2002**, *12*, 255−271.
(21) Rosenzweig, A. C.; Huffman, D. L.; Hou, M. Y.; Wernimont, A. K.; Pufahl, R. A.; O'Halloran, T. V. *Structure (Cambridge, MA, U.S.)* **1999**, *7*, 605−617.
(22) Wimmer, R.; Herrmann, T.; Solioz, M.; Wüthrich, K. *J. Biol. Chem.* **1999**, *274*, 22597−22603.
(23) Wernimont, A. K.; Huffman, D. L.; Lamb, A. L.; O'Halloran, T. V.; Rosenzweig, A. C. *Nat. Struct. Biol.* **2000**, *7*, 766−771.
(24) Banci, L.; Bertini, I.; Del Conte, R.; Markey, J.; Ruiz-Duenas, F. J. *Biochemistry* **2001**, *40*, 15660−15668.
(25) Banci, L.; Bertini, I.; Ciofi-Baffoni, S.; Huffman, D. L.; O'Halloran, T. V. *J. Biol. Chem.* **2001**, *276*, 8415−8426.
(26) Opella, S. J.; DeSilva, T. M.; Veglia, G. *Curr. Opin. Struct. Biol.* **2002**, *6*, 217−223.
(27) Steele, R. A.; Opella, S. J. *Biochemistry* **1997**, *36*, 6885−6895.
(28) Banci, L.; Bertini, I.; Ciofi-Baffoni, S.; Finney, L. A.; Outten, C. E.; O'Halloran, T. V. *J. Mol. Biol.* **2002**, *323*, 883−897.
(29) Hou, Z.-j.; Narindrasorasak, S.; Bhushan, B.; Sarkar, B.; Mitra, B. *J. Biol. Chem.* **2001**, *276*, 40858−40863.
(30) Hou, Z.; Mitra, B. *J. Biol. Chem.* **2003**, *278*, 28455−28461.
(31) Veglia, G.; Porcelli, F.; DeSilva, T.; Prantner, A.; Opella, S. J. *J. Am. Chem. Soc.* **2000**, *122*, 2389−2390.
(32) Urvoas, A.; Moutiez, M.; Estienne, C.; Couprie, J.; Mintz, E.; Le Clainche, L. *Eur. J. Biochem.* **2004**, *271*, 993−1003.
(33) Jiang, J.; Nadas, I. A.; Kim, M. A.; Franz, K. J. *Inorg. Chem.* **2005**, *44*, 9787−9794.
(34) Xing, G.; DeRose, V. J. *Curr. Opin. Chem. Biol.* **2001**, *5*, 196−200.
(35) Ghosh, D.; Pecoraro, V. L. *Inorg. Chem.* **2004**, *43*, 7902−7915.
(36) Ghosh, D.; Lee, K.-H.; Demeler, B.; Pecoraro, V. L. *Biochemistry* **2005**, *44*, 10732−10740.
(37) Kharenko, O. A.; Ogawa, M. *J. Inorg. Biochem.* **2004**, *98*, 1971−1974.
(38) Payne, J. C.; ter Horst, M. A.; Godwin, H. A. *J. Am. Chem. Soc.* **1999**, *121*, 6850−6855.
(39) Sénèque, O.; Crouzy, S.; Boturyn, D.; Dumy, P.; Ferrand, M.; Delangle, P. *Chem. Commun.* **2004**, 769−770.

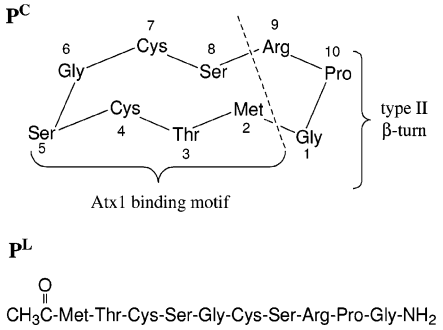

Figure 1. Peptides P^C and P^L.

ions with a selectivity for Hg(II) and Cu(I) over Pb(II), Cd(II), and Zn(II). Moreover, the solution structures of the apo and Hg-loaded forms of this cyclodecapeptide showed that it is an excellent structural model of the binding loop of the copper chaperone Atx1, especially the Hg complex, which reproduces both the binding mode and the second-coordination-sphere interactions observed in the X-ray structure of the Hg(II)-loaded form of Atx1.[21] In this complex, Hg is bound to the peptide by the two cysteine S atoms in a linear arrangement and the second-sphere interactions around the metal ion are also well-reproduced: each S atom of the cysteine is H-bonded to an amide NH donor of the peptidic backbone and an O atom lies at ~3 Å of the Hg ion.

Here we report on an extensive analysis of the metal binding properties of this cyclic peptide for Hg(II), Cu(I), Pb(II), Cd(II), and Zn(II). To test the effect of the β turn induced by the xPGx motif in the cyclic peptide, we have compared the complexation behavior of P^C with that of the corresponding linear peptide P^L shown in Figure 1. The coordination properties of the two peptides were investigated by means of complementary analytical and spectroscopic methods, and the affinities were determined for the series of outlined metal cations.

The results presented in this Article show that the overall behaviors of the two peptide/metal complexes are similar. Nevertheless, the stabilities of the complexes obtained with the cyclic compound are systematically higher than those observed with the linear one, which exemplifies a small stabilization of the complexes formed with the slightly preorganized peptide P^C. The selectivity of the consensus sequence MxCxxC found in many heavy-metal transporters has been measured to be Hg(II) > Cu(I) ≫ Cd(II) > Pb(II) > Zn(II).

Experimental Section

Peptide Synthesis and Purification. (a) Abbreviations: Ac_2O, acetic anhydride; DMF, *N*,*N*-dimethylformamide; DIEA, *N*,*N*-diisopropylethylamine; EDT, ethanedithiol; Et_2O, diethyl ether; Fmoc, 9-fluorenylmethyloxycarbonyl; PyBOP, (benzotriazole-1-yloxy)tris(pyrrolidino)phosphonium hexafluorophosphate; TFA, trifluoroacetic acid; TIS, triisopropylsilane; TNBS, 2,4,6-trinitrobenzenesulfonic acid.

(b) c(GMTCSGCSRP) (P^C). The linear precursor with protected side chains HCys(Trt)-Ser(*t*-Bu)-Arg(Pbf)-Pro-Gly-Met-Thr(*t*-Bu)-Cys(Trt)-Ser(*t*-Bu)-GlyOH was assembled manually by solid-phase peptide synthesis on 2-chlorotrityl resin (substitution 0.6 mmol g^{-1}, 400 mg) using Fmoc chemistry. Couplings were performed with N-α-Fmoc-protected amino acids (2 equiv), PyBOP (2 equiv), and DIEA (pH ≈ 8−9) in DMF. The coupling reaction was monitored by a TNBS test.[40] For noncomplete reactions, a second coupling was achieved, followed by 7:2:1 DMF/pyridine/Ac_2O treatment. Fmoc deprotection was achieved with 4:1 DMF/piperidine. The peptide was cleaved from the resin by treatment with 98:2 CH_2Cl_2/TFA for 2 h. After concentration, the residue was precipitated in cold diethyl ether. The linear precursor was then reacted in DMF (0.5 mM) with PyBOP (3.5 equiv) and DIEA (pH ≈ 8−9) for 3 h. DMF was evaporated under reduced pressure. The oily residue was precipitated with CH_2Cl_2/Et_2O to yield the cyclic peptide as a powder. Removal of side-chain protecting groups was performed in TFA/TIS/H_2O/EDT (90:2.5:2.5:5). After 2 h of stirring, the solution was evaporated to yield a yellow oil, which was washed with Et_2O. The solid residue was dissolved in water/acetonitrile and purified by reversed-phase high-performance liquid chromatography (RP-HPLC; Delta pack 300-Å, 15-μm C18 particles, 200 × 25 mm, solvent A = 99.9:0.1 H_2O/TFA, solvent B = 90:10:0.1 CH_3CN/H_2O/TFA, flow rate 22 mL min^{-1}) to yield c(GMTCSGCSRP) as a white powder (52 mg, 17% overall yield). Analytical RP-HPLC was performed using an analytical column (Nucleosil 120-Å, 3-μm C18 particles, 30 × 4.6 mm) at 1.3 mL min^{-1} with UV monitoring at 214 nm. t_R = 5.78 min (gradient 5−100% of B in 15 min). ESMS: *m*/*z* 980.3 [M + H].

(c) Ac-MTCSGCSRPG-NH_2 (P^L). P^L was assembled manually in a similar way on Rink Amide MBHA resin. After the last Fmoc removal, the peptide was acetylated by treatment with 7:2:1 DMF/pyridine/Ac_2O. Cleavage and removal of side-chain protecting groups were performed in TFA/TIS/H_2O/EDT (90:2.5:2.5:5). t_R =5.73 min (gradient 5−100% of B in 15 min). ESMS: *m*/*z* 1039.4 [M + H].

Sample Preparation. Fresh solutions of the purified peptide were prepared before each experiment, using deoxygenated Milli-Q water (Millipore) containing 20 mM of the appropriate buffer. The final concentration of the peptide solution was determined by measuring the cysteine free thiol concentration following Ellman's procedure.[41] This UV/visible procedure uses 5,5′-dithiobis-2-nitrobenzoic acid as an indicator; each free thiol group present in the peptide yields 1 equiv of TNB^{2-} [$\epsilon^{412\ nm}(TNB^{2-})$ = 14 150 M^{-1} cm^{-1}]. The concentrations of the peptide solution range from 30 to 100 μM for UV titrations and from 1 to 3 mM for NMR experiments.

Metal solutions [except Cu(I)] were prepared from the corresponding salt ($HgCl_2$, $CdCl_2$, $PbCl_2$, or $ZnCl_2$) in the appropriate buffer and titrated by 5 mM volumetric ethylenediaminetetraacetic acid (Fisher Chemicals) in the presence of a colorimetric indicator.

Cu(I) solutions were prepared before each experiment by dissolving the appropriate amount of $Cu(CH_3CN)_4PF_6$ in deoxygenated acetonitrile. The final concentration was determined by adding an excess of sodium bathocuproine disulfonate (Na_2bcs) and measuring the absorbance of $Cu(bcs)_2^{3-}$ (λ_{max} = 483 nm; ϵ = 13 300 M^{-1} cm^{-1}).

NMR. All of the NMR experiments were recorded on a 500-MHz Bruker Avance spectrometer equipped with a BBI probe with a triple-axis gradient field. ^1H NMR spectra were recorded with 12 ppm windows and 32K data points in the time domain. 2D ^1H NMR spectra of P^C_{SS} (2 mM) were recorded at 298 K in 9:1 H_2O/D_2O using Watergate[42,43] or presaturation solvent suppression. 2D

(40) Hancock, W. S.; Battersby, J. E. *Anal. Biochem.* **1976**, *71*, 260−264.
(41) Riddles, P. W.; Blakeley, R. L.; Zerner, B. *Methods Enzymol.* **1983**, *91*, 49−60.

spectra were acquired in phase-sensitive mode with TPPI for quadrature detection in the indirect dimension, using 2048 × 256 (TOCSY) or 2048 × 512 (t-ROESY) matrices over a 5000-Hz spectral width. TOCSY experiments were performed using a MLEV-17[44] spin-lock sequence with a mixing time of 70 ms. t-ROESY[45,46] experiments were recorded with a mixing time of 300 ms (3300-Hz spin lock). Soft-COSY[47] experiments (256 × 128) were acquired using 20-ms self-refocusing 270°[48] selective pulses with a Gaussian envelope and a 100-Hz spectral width.

(a) Structure Calculation. Solution structures were calculated using the program *X-PLOR* 3.1 following standard refinement protocols.[49] Upper and lower limits for distance constraints were set to ±10% of the H−H distances obtained by integration of ROESY spectra (200 ms). Φ dihedral constraints were derived from $^3J_{HN,H\alpha}$ coupling constants measured on ^{1}H NMR spectra or by soft-COSY experiments. Pseudo-atom corrections were applied to methyl and nonstereospecifically assigned methylenes.[50] Gly Hα1/Hα2 (1.78 Å), Pro Hβ1/Hβ2 (1.78 Å), Pro Hγ1/Hγ2 (1.78 Å), Pro Hα/Hβ1 (2.36 Å), and Pro Hα/Hβ2 (2.70 Å) were used as references for distance calibrations. No nuclear Overhauser effect violations greater than 0.5 Å and no dihedral angle violations greater than 5° were found.

(b) Diffusion Coefficient Measurement. The diffusion experiments were performed using the bipolar stimulated spin−echo sequence.[51] Diffusion coefficients were obtained using $I(\delta,\Delta,g) = I_0 \exp[-\gamma^2 g^2 \delta^2(\Delta - \delta/3)D]$, where $I(\delta,\Delta,g)$ and I_0 are the intensities in the presence of gradient pulses of strength g and in the absence of gradient pulses, respectively. The length of the gradient pulse is δ, Δ is the diffusion delay, and γ is the gyromagnetic ratio (for protons, $\gamma = 26.7520 \times 10^7$ rad T^{-1} s^{-1}). The values of Δ and δ used in the diffusion coefficient measurements were 96 and 2 ms, respectively. In the experiments, g was incremented from 3.3 to 52.8 G cm^{-1}.

Electrospray Ionization Mass Spectrometry (ESMS). Mass spectra were acquired on a LCQ ion trap (Finnigan-Thermoquest, San Jose, CA) equipped with an electrospray source. Electrospray full-scan spectra in the range m/z 150−2000 or 2000−3000 were obtained by infusion through a fused-silica tubing at 2−10 μL min^{-1}. The solutions were analyzed in the positive mode. The LCQ calibration (m/z 50−2000) was achieved according to the standard calibration procedure from the manufacturer (mixture of caffeine, MRFA, and U1-tramark 1621). An ES-Tuning Mix solution (Agilent) was used to calibrate the spectrometer between 2000 and 3000 amu. The temperature of the heated capillary for the LCQ was set to 180 °C, the ion-spray voltage was in the range 4−6 kV, and the injection time was 5−200 ms.

Size-Exclusion Chromatography (SEC). The apopeptides and their complexes with Hg(II), Zn(II), Cd(II), and Pb(II) were subjected to SEC in order to estimate their molecular weights. These experiments were performed with a Merck Instrument equipped with an Amersham Biosciences Superdex PC 3.2/30 size-exclusion column (3.2 × 300 mm) under isocratic conditions. The flow rate was 50 μL min^{-1}, and the separation was followed spectrophotometrically at 220 nm. Molecular weights were estimated from a calibration plot derived from Aprotinin (6500 g mol^{-1}), Gastrin I (2126 g mol^{-1}), and Substance P (1348 g mol^{-1}) (all Sigma reagents), and the plot is given in Figure S1 in the Supporting Information. A total of 10 μL of the peptides and complexes was injected at a concentration of 0.2 mM. The chromatogram of the peptide that we obtained in those conditions displayed a broad peak corresponding to the peptide and other species of higher molecular weight assumable to oxidation during the elution process. The elution of the Hg complex, prepared by the addition of 1 equiv of $HgCl_2$ to the peptide solution, did not show this broad signal but only a single peak corresponding to the molecular weight of the complex, showing no oxidation of the Hg complex due to its high stability. In the following experiments, we used a reducing agent (TCEP) to avoid any oxidation of the cysteine during the elution process. All of the complexes were eluted at the same concentration, in the presence of 5-fold excess of metal in the buffer solution, to prevent any disruption of the complexes during the elution process. The buffer was phosphate (20 mM, pH 7) containing 100 mM NaCl, except for Pb(II), for which phosphate was replaced by Bis-Tris (20 mM, pH 7). In this latter case, separation was followed at 315 nm.

P^C: calcd, 980; found, 1200. $M^{II}P^C$: calcd, 1043−1180; found, 1100−1400.

P^L: calcd, 1039; found, 1300. $M^{II}P^L$: calcd, 1100−1239; found, 1100−1500.

UV/Visible Spectroscopy. All of the UV/visible titrations were performed with a Varian Cary 50 spectrophotometer. A total of 2.5 mL of the freshly prepared peptide solution was transferred in a UV cell (1-cm path length) sealed with a septum. Aliquots corresponding to 0.1 equiv of the metal solution in the selected buffer were then added with an airtight syringe (Hamilton) via the septum, to avoid any oxidation of the thiol groups. For Cu(I) titrations, a solution of tetrakis(acetonitrile)copper(I) hexafluorophosphate dissolved in acetonitrile was added.

For back-titrations, aliquots of Cd(II) or Zn(II) solutions in 20 mM Bis-Tris were added to the UV cell containing the peptide/Pb complex in Bis-Tris (20 mM, pH 7), made of 1 equiv of peptide and 5 equiv of Pb(II). The experiment was performed until no signal of the peptide/Pb complex could be observed, or less than 10%.

Spectra were analyzed using the program SPECFIT,[52−55] which employs a singular value decomposition algorithm and refines the data according to a global least-squares analysis procedure. The buffer (Bis-Tris) was selected because it forms a stable, soluble complex with Pb(II) and thereby prevents the formation and precipitation of $Pb(OH)_2$.[38] The affinities of the metal ions for Bis-Tris are known and were included as parameters in the fit [log β_1 = 2.47 for Cd(II), 2.38 for Zn(II), and 4.32 for Pb(II)].[56] The Pb(Bis-Tris) complex only weakly absorbs in the region 250−400 nm; nonetheless, the spectrum of Pb(Bis-Tris) was included as a

(42) Piotto, M.; Saudek, V.; Sklenar, V. *J. Biomol. NMR* **1992**, *2*, 661−665.
(43) Sklenar, V.; Piotto, M.; Leppik, R.; Saudek, V. *J. Magn. Reson. A* **1993**, *102*, 241−245.
(44) Bax, A.; Davis, D. G. *J. Magn. Reson.* **1985**, *65*, 355−360.
(45) Desvaux, H.; Berthault, P.; Birlirakis, N.; Goldman, M.; Piotto, M. *J. Magn. Reson. A* **1995**, *113*, 47−52.
(46) Malliavin, T. E.; Desvaux, H.; Delsuc, M.-A. *Magn. Reson. Chem.* **1998**, *36*, 801−806.
(47) Brüschweiler, R.; Madsen, J. C.; Griesinger, C.; Sørensen, O. W.; Ernst, R. R. *J. Magn. Reson.* **1987**, *73*, 380−385.
(48) Emsley, L.; Bodenhausen, G. *J. Magn. Reson.* **1989**, *82*, 211−221.
(49) Brünger, A. T. A system for X-ray Crystallography and NMR. *X-PLOR*, version 3.1; Yale University Press: New Haven, CT, 1992.
(50) Fletcher, C. M.; Jones, D. N. M.; Diamond, R.; Neuhaus, D. *J. Biomol. NMR* **1996**, *8*, 292−310.
(51) Jershow, A.; Müller, N. *J. Magn. Reson.* **1997**, *125*, 372−375.
(52) Gampp, H.; Maeder, M.; Meyer, C. J.; Zuberbühler, A. D. *Talanta* **1985**, *32*, 95−101.
(53) Gampp, H.; Maeder, M.; Meyer, C. J.; Zuberbühler, A. D. *Talanta* **1985**, *32*, 257−264.
(54) Gampp, H.; Maeder, M.; Meyer, C. J.; Zuberbühler, A. D. *Talanta* **1985**, *32*, 1133−1139.
(55) Gampp, H.; Maeder, M.; Meyer, C. J.; Zuberbühler, A. D. *Talanta* **1986**, *33*, 943−951.
(56) Scheller, K. H.; Abel, T. H.; Polanyi, P. E.; Wenk, P. K.; Fischer, B. E.; Sigel, H. *Eur. J. Biochem.* **1980**, *107*, 455−466.

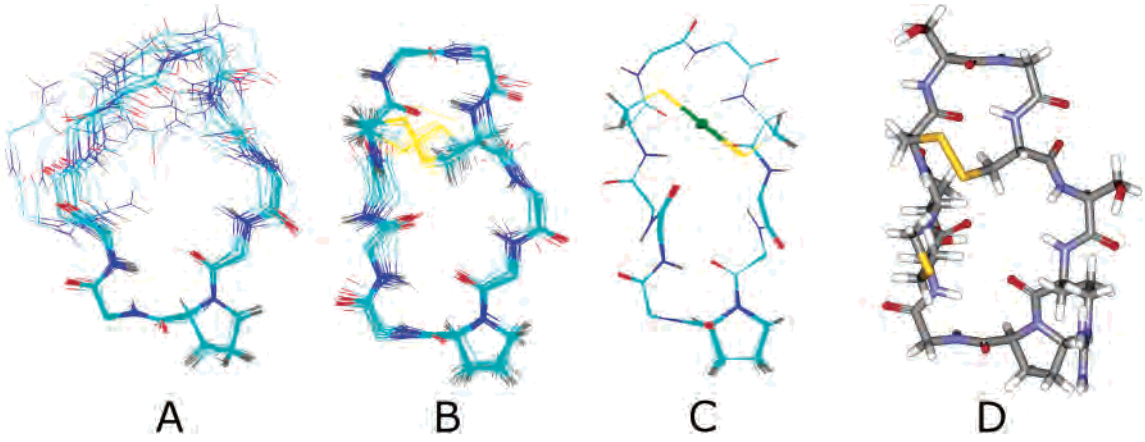

Figure 2. NMR solution structures calculated using *X-PLOR*: (A−C) Superposition of the 20 lowest-energy structures of (A) P^C, (B) P^C_{SS}, and (C) HgP^C. The side chains of Cys4, Cys7 (B and C only), and Pro10 are displayed. (D) Lowest-energy structure of P^C_{SS}.

known spectrum in the fitting procedure. The stability constants of Pb(II)/peptide complexes were included as parameters in the fit of the back-titrations with Cd(II) and Zn(II).

For the titrations of Cu(I)-loaded peptides with bcs, the complex was freshly prepared by adding 0.9 equiv of the Cu(I) solution in acetonitrile to the peptide solution in Bis-Tris (20 mM, pH 7). The mixture was stirred for 10 min under Ar to ensure the formation of the complex. Aliquots of bcs [in Bis-Tris (20 mM pH 7)] were then added via an airtight syringe to the Cu/peptide complex. The UV/visible spectra were recorded after 30 min of stirring, and the stability of the absorbance was controlled before the addition of any other aliquots. The UV/visible titrations were analyzed with SPECFIT. The affinity of $Cu(bcs)_2^{3-}$ is known and was introduced into the fit ($\log \beta = 19.8$).

Results

Synthesis and Characterization of the Apopeptides. Classical solid-phase synthesis using Fmoc/*t*-Bu strategy was used for the synthesis of the two peptides. The linear compound P^L is acetylated at the N terminus and amidated at the C terminus. For the cyclic peptide P^C, the 10-mer-protected linear precursor H-Cys(Trt)-Ser(*t*-Bu)-Arg(Pbf)-Pro-Gly-Met-Thr(*t*-Bu)-Cys(Trt)-Ser(*t*-Bu)-Gly-OH was assembled on the resin and cyclized in DMF after cleavage from the resin. The side chains were subsequently deprotected.

The solution structures of apo-P^C and -P^L were investigated by 1D and 2D ^{1}H NMR experiments in H_2O/D_2O (2 mM, 298 K, 500 MHz). The NMR data obtained for the cyclic compound P^C show that the RPGM region is well-defined whereas the binding loop is rather flexible (see Figure 2A).[39] This reproduces well the flexibility of the solvent-exposed loop observed in the apoprotein Atx1.[14] P^L resonances in the HN and Hα regions are clearly less dispersed than those of P^C. For the linear peptide, the two enantiotopic α protons of the glycines are not differentiated and the 2D t-ROESY spectrum shows very few interresidue correlations. As expected, these data indicate that the linear compound does not adopt any preferential conformation.

The peptides are stable in aqueous solutions stored anaerobically but are oxidized in the presence of air. P^C could be slowly oxidized by air in water into the corresponding disulfide peptide P^C_{SS} (starting pH 5.5, 2 days at 50 °C for complete conversion). The solution structure of P^C_{SS} was investigated by ^{1}H NMR experiments in 9:1 H_2O/D_2O (2.5 mM, 298 K, 500 MHz). It displays the same characteristic elements of the type II β turn for the RPGM motif as for P^C. However, five $^3J_{HN,H\alpha}$ values out of the 6−8-Hz range were observed along the backbone (all of them were in the 6−8-Hz range for P^C), showing that the peptide adopts a well-defined conformation. Characteristic elements of another type II β turn were also observed for the CSGC motif [d(Cys4 Hα,Ser5 HN) = 2.2 Å, d(Gly6 HN,Ser5 Hα) = 2.1 Å, d(Gly6 HN,Cys7 HN) = 2.6 Å, and d(Cys7 HN,Ser5 Hα) = 3.4 Å] and $^3J_{HN,H\alpha}$(Ser5) = 4.5 Hz corresponding to $-90° < \Phi < -40°$.[57] A similar type II β turn was observed in the X-ray structure of the oxidized Atx1.[21] This stands in contrast with the Hg-loaded forms of Atx1 and P^C, displaying rather a type I β turn for the CSGC motif, which allows the formation of a H bond between Gly NH and the cysteine S atoms. No such H bonds are observed in the disulfide forms either of Atx1 or of our model peptide. A superposition of the 20 lowest-energy structures calculated using *X-PLOR* with the NMR-derived constraints (Figure 2B) shows that P^C_{SS} adopts a unique conformation (Figure 2D) with a backbone root-mean-square deviation (RMSD) of 0.55 Å (overall RMSD: 1.66 Å). Although the cysteine side chains adopt different conformations among these structures, the disulfide bridge between Cys4 and Cys7 clearly rigidifies the whole peptide backbone compared to P^C. Finally, the Hg(II) complex appears to be the most rigid (Figure 2C). This is probably due to the second-sphere interactions [two H bonds between backbone NH and S atoms (Cys4 S···HN−Gly6 and Cys7 S···HN−Arg8) and a Thr3 CO···Hg interaction], which lock the peptide into a unique conformation.

Divalent Cation [Hg(II), Pb(II), Cd(II), and Zn(II)] Complexes of P^C and P^L. (a) Mass Spectrometry. The formation of the metal complexes of peptides P^C and P^L was followed by ESMS. Whereas Hg(II) adducts are directly detected in water, the complexation of Cd(II), Pb(II), and Zn(II) needs the addition of an exogenous base to promote the deprotonation of the thiol functions of the two cysteines.

(57) Wüthrich, K.; Billeter, M.; Braun, W. *J. Mol. Biol.* **1984**, *180*, 715−740.

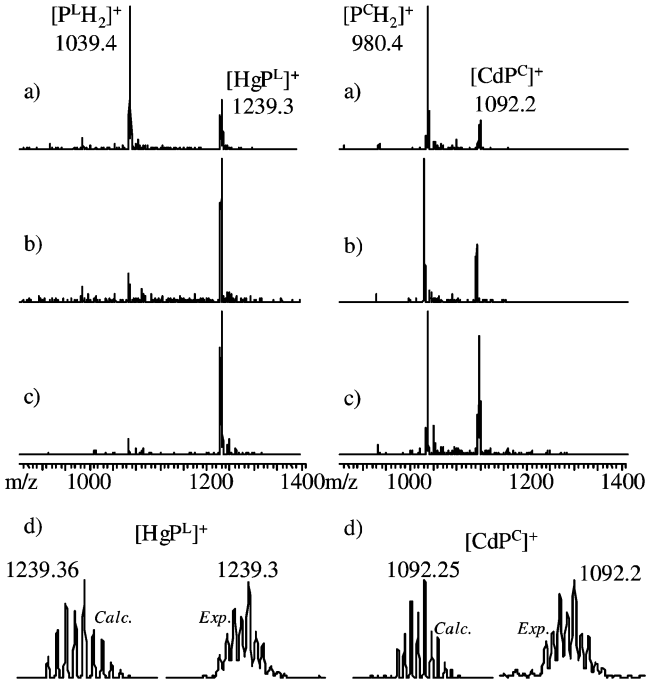

Figure 3. ESMS spectra in the positive mode. Left: $HgCl_2$ with P^L in water at (a) 0.5:1, (b) 1:1, and (c) 2:1 and (d) calculated and experimental isotopic patterns of the complex. Right: $CdCl_2$ with P^C in an ammonium acetate buffer (20 mM, pH 6.9) at (a) 0.5:1, (b) 1:1, and (c) 2:1 and (d) calculated and experimental isotopic patterns of the complex.

Table 1. Ions Detected in the ESMS Spectra (Positive Mode) of the Complexes with P^C and P^L

	m/*z*			*m*/*z*	
	P^C	P^L		P^C	P^L
$(PH_2)^+$	980.4	1039.4	$(PbP)^+$	1186.2	1245.3
$(HgP)^+$	1180.3	1239.3	$(ZnP)^+$	1044.2	1101.2
$(CdP)^+$	1092.2	1151.2			

Therefore, the mass spectra for these three cations were recorded in an ammonium acetate buffer at pH 6.9. Typical titrations are presented in Figure 3 for HgP^L and CdP^C and show that the signal of the complex increases as a function of the metal concentration in the sample. With Hg complexes, the signal of the free peptides disappears and is fully converted into the signal of the Hg-loaded peptides $[HgP^C]^+$ at *m*/*z* 1180 and $[HgP^L]^+$ at *m*/*z* 1239, above 1 equiv of cation. On the contrary, with Cd(II), Pb(II), and Zn(II), the free peptides always represent the major signal in the ESMS spectra even in a 2-fold excess of the metal cation. In all cases, only monocharged ions $[MP]^+$ are detected, characteristic of a 1:1 peptide/metal stoichiometry. The *m*/*z* values measured in the mass spectra are given in Table 1.

(b) UV−Visible Spectroscopy. The binding of metal cations with the two peptides P^C and P^L was monitored using the ligand-to-metal charge-transfer (LMCT) bands for Hg−S, Cd−S, and Pb−S bonds in the UV spectral window. To distinguish these metal-centered bands from the UV absorption of the peptide, difference spectra were taken by subtracting a background of peptide in the absence of metal. Extinction coefficients for the LMCT bands were calculated on the basis of the total metal concentration. All titrations reveal complete binding at a 1:1 metal/peptide stoichiometry. Band maxima and extinction coefficients are collected in Table 2.

Table 2. LMCT Band Characteristics for Hg(II), Cd(II), Pb(II), and Cu(I) Complexes with P^C and P^L

	P^C		P^L	
	λ (nm)	$\Delta\epsilon$ (M^{-1} cm^{-1})	λ (nm)	$\Delta\epsilon$ (M^{-1} cm^{-1})
HgP^a	220	12500	220	12450
	250	1300	250	1200
CdP^a	221	13000	225	10000
$Cd(P)_2{}^a$	240	25000	240	20000
PbP^b	315	3100	315	3300
$Pb(P)_2{}^b$	335	4000	340	5200
$Cu(P)^b$	261	8800	261	8600

[a] Phosphate buffer (20 mM, pH 7). [b] Bis-Tris buffer (20 mM, pH 7).

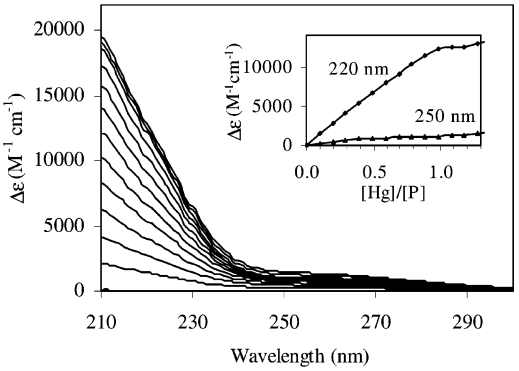

Figure 4. UV titration of P^C (52 μM) with mercury chloride at pH 7 (20 mM phosphate buffer). Spectra shown are difference spectra [$\Delta\epsilon = \epsilon(HgP^C) - \epsilon(P^C)$] and correspond to samples with 0−1.3 equiv of Hg(II) per P^C. The inset shows $\Delta\epsilon$ at 220 and 250 nm vs equiv of Hg(II) per P^C.

Figure 4 illustrates the typical difference absorption spectra for the titration of Hg(II) into a solution of P^C at pH 7. The wavelength and extinction coefficient for the major transition are similar to those observed for linear bis(thiolate)mercury(II) complexes.[58,59] Indeed the absorbance maximum for the $Hg(S)_2$ LMCT band is below 220 nm with an extinction coefficient of around 12 000 M^{-1} cm^{-1} at 220 nm and 1000 M^{-1} cm^{-1} at 250 nm. Hg(II) saturates the peptide at 1 mol equiv, suggesting that a 1:1 complex is formed. These data are consistent with the ^{199}Hg NMR chemical shift measured for the complex HgP^C (−937 ppm), which is typical of a linear bicoordinate Hg(II) with thiolate ligands.[39,58,60] The linear evolution of $\Delta\epsilon$ as a function of the metal-to-ligand ratio up to 1 equiv is consistent with the formation of only one complex (1:1) without any intermediate of the type $Hg(P)_2$ having a trigonal or tetragonal coordination for Hg(II). The data are similar to those of P^L. Nevertheless, the evolution of the absorbance at 250 nm, which is not linear between 0 and 1 equiv of Hg, may indicate the formation of HgS_3 or HgS_4 adducts in excess of peptide. Furthermore, after 1 equiv of Hg(II), the absorbance is still slightly

(58) Diekmann, G. R.; McRorie, D. K.; Tierney, D. L.; Utschig, L. M.; Singer, C. P.; O'Halloran, T. V.; Penner-Hahn, J. E.; DeGrado, W. F.; Pecoraro, V. L. *J. Am. Chem. Soc.* **1997**, *119*, 6195−6196.
(59) Matzapetakis, M.; Farrer, B. T.; Weng, T.-C.; Hemmingsen, L.; Penner-Hahn, J. E.; Pecoraro, V. L. *J. Am. Chem. Soc.* **2002**, *124*, 8042−8054.
(60) Utschig, L. M.; Bryson, J. W.; O'Halloran, T. V. *Science* **1995**, *268*, 380−385.

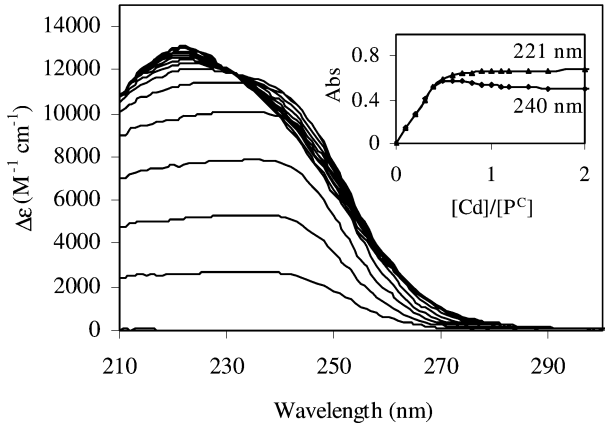

Figure 5. UV titration of P^C (53 μM) with cadmium chloride at pH 7 (20 mM phosphate buffer). Spectra shown are difference spectra [$\Delta\epsilon = \epsilon(CdP^C) - \epsilon(P^C)$] and correspond to samples with 0−1.6 equiv of Cd(II) per P^C. The inset shows the absorbance at 221 and 240 nm vs equiv of Cd(II) per P^C.

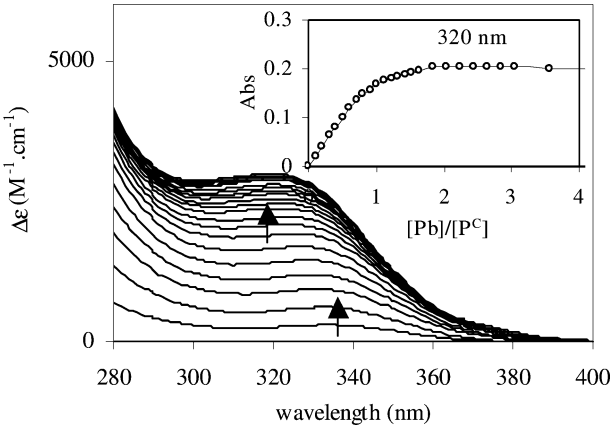

Figure 6. UV titration of P^C (73 μM) with lead chloride at pH 7 (20 mM Bis-Tris). Spectra shown are difference spectra [$\Delta\epsilon = \epsilon(PbP^C) - \epsilon(P^C)$] and correspond to samples with 0−3 equiv of Pb(II) per P^C. The inset shows calculated (line) and experimental (circles) absorbances at 320 nm. Calculated lines have been generated in SPECFIT, with the stability constants of Pb(II) complexes reported in Table 3.

growing, which may be characteristic of the formation of oligomeric complex species (see Figure S2 in the Supporting Information).

A similar titration with cadmium chloride is shown in Figure 5. In this case, two successive charge-transfer bands are observed. At the beginning of the titration, when [Cd]/[P] < 0.5, a first LMCT band is detected with a maximum absorption λ_{max} at 240 nm and an extinction coefficient of 25 000 M^{-1} cm^{-1}. These values are consistent with a CdS_4 environment for Cd(II). Indeed, it has been demonstrated that the intensity of the lowest-energy CysS−Cd(II) LMCT band is proportional to the number of cysteine ligands involved in metal binding: ≈6000 M^{-1} cm^{-1} per cysteine thiolate.[61] This first species thus corresponds to the complex $Cd(P^C)_2$. Then, as more Cd is added, a second higher-energy band develops with a λ_{max} at 221 nm and an extinction coefficient of 13 000 M^{-1} cm^{-1}, indicative of a lower number of coordinated thiolates per Cd atom. Cd(II) saturates the peptide at 1 mol equiv. These data are consistent with the coordination of two thiolates per Cd ion and thus to the complex $Cd(P^C)$. The results of Cd(II) binding titration of the linear peptide P^L are very similar (see Figure S3 in the Supporting Information) and also indicate the formation of two successive complexes according to eqs 1 and 2.

$$M(II) + 2P = M(P)_2 \qquad \log \beta_{12} \qquad (1)$$

$$M(II) + P = MP \qquad \log \beta_{11} \qquad (2)$$

The results of a representative Pb(II) binding titration of P^C are shown in Figure 6. Pb−S charge-transfer transitions arise at higher wavelengths than those detected for Cd−S and Hg−S charge-transfer transitions. The low-energy Pb−S transitions are observed above 250 nm and are not obscured by absorbance of the Bis-Tris buffer, which was selected because it forms a stable, soluble complex with Pb(II).[38,62] As for Cd(II), two complexes are formed with Pb(II): the first band appears with a maximum absorption λ_{max} at 335 nm and an extinction coefficient of 4000 M^{-1} cm^{-1}. These spectroscopic characteristics are consistent with three or four thiolate ligands bound to Pb(II) and thus with a $Pb(P^C)_2$ species. Indeed, S-rich proteins or peptides containing three or four cysteines give ligand-to-Pb charge-transfer bands at ≈330 nm with an extinction coefficient of 4000 M^{-1} cm^{-1}.[38,62,63] The second band has a higher energy with a λ_{max} at 315 nm and an extinction coefficient of 3100 M^{-1} cm^{-1}, which is very similar to the spectroscopic data of a Pb complex with a Zn finger peptide that contains two cysteines and two histidines.[38] This second species corresponds to $Pb(P^C)$, where Pb is coordinated to two thiolates only. The binding of the linear and cyclic peptides P^L and P^C to Pb(II) give similar spectra and can also be described with eqs 1 and 2.

The UV titrations described above clearly demonstrate that ML and ML_2 complexes are formed with Cd(II) and Pb(II), whereas only 1:1 complexes are detected in the ESMS spectra. This shows that ESMS is not totally reliable in this case to unambiguously evidence the nature of the complexes formed. Thiolate/metal systems have a great tendency to form dimeric or polymeric structures. Indeed, previous studies of similar metal cysteine/peptide systems have shown that dimeric complexes M_2L_2 can be obtained.[64,65] Therefore, we decided to investigate the molecularity of the complexes by SEC.

(61) Henehan, C. J.; Poutney, D. L.; Zerbe, O.; Vasak, M. *Protein Sci.* **1993**, *2*, 1756−1764.

(62) Magyar, J. S.; Weng, T.-C.; Stern, C. M.; Dye, D. F.; Rous, B. W.; Payne, J. C.; Bridgewater, B.; Mijovilovich, A. M.; Parkin, G.; Zaleski, J. M.; Penner-Hahn, J. E.; Godwin, H. A. *J. Am. Chem. Soc.* **2005**, *127*, 9495−9505.

(63) Ghering, A. B.; Miller-Jenkins, L. M.; Schenck, B. L.; Deo, S.; Mayer, R. A.; Pikaart, M. J.; Omichinski, J. G.; Godwin, H. A. *J. Am. Chem. Soc.* **2005**, *127*, 3751−3759.

(64) Nivorozhkin, A. L.; Segal, B. M.; Musgrave, K. B.; Kates, S. A.; Hedman, B.; Hodgson, K. O.; Holm, R. H. *Inorg. Chem.* **2000**, *39*, 2306−2313.

(65) Ciuculescu, E.-D.; Mekmouche, Y.; Faller, P. *Chem.—Eur. J.* **2005**, *11*, 903−909.

Table 3. Apparent Equilibrium Constants (log β_{pq}) at pH 7 and 298 K in 20 mM Bis-Tris ($\beta_{pq} = [M_pP_q]/[M]^p[P]^q$)

M	log β_{pq}	P^C	P^L
Pb(II)	log β_{11}	8.0(1)	7.5(2)
	log β_{12}	12.5(7)	11.6(1)
Cd(II)	log β_{11}	9.2(1)	8.3(2)
	log β_{12}	15.6(1)	14.8(6)
Zn(II)	log β_{11}	6.8(2)	6.3(3)
	log β_{12}	13.0(5)	12.2(1)
Hg(II)	log β_{11}[a]	>18.6	>18.4
Cu(I)	log β_{11}	16.6(1)	16.4(1)

[a] log $\beta(P^C)$ − log $\beta(P^L) \geq 2$.

(c) SEC. SEC−HPLC experiments have been performed for complexes of P^C and P^L with Hg(II), Cd(II), Pb(II), and Zn(II) to discriminate between monomeric and polymeric complexes. The apopeptides elute with apparent masses of 1200 g mol^{-1} (P^C) and 1300 g mol^{-1} (P^L), compatible with the mass of the monomers. In all cases, the elution volumes of the complexes were comparable to those obtained for the apopeptide. The complexes obtained at the end of the UV titrations are thus unambiguously monomeric adducts MP, with only two thiolates coordinated to the cation, the coordination sphere of which may be completed with anions or buffer molecules.

(d) Affinity Constants. The stability constants of the complexes identified above were measured in Bis-Tris (20 mM) at pH 7 and 25 °C. The Bis-Tris buffer was selected because it forms weak complexes with Zn(II), Pb(II), and Cd(II) with known affinities that could be inserted in the fitting procedure.[56,66] Furthermore, it prevents the formation and precipitation of $Pb(OH)_2$. Pb binding constants were determined from the absorption spectra for the direct titration of the peptides with lead chloride. Factor analysis performed with the program SPECFIT[52−55] confirms the existence of three absorbing species: two complexes formed with the peptide [Pb(P) and $Pb(P)_2$] and the adduct with the buffer Pb(Bis-Tris). The spectrophotometric data were satisfactorily fitted with eqs 1 and 2, allowing an estimation of the overall stability constants of Pb/peptide complexes in solution for P^C and P^L (Table 3).

Similar direct titrations with Cd(II) show only a small part of the LMCT band as Bis-Tris absorbs below 250 nm. Attempts to fit these spectroscopic data gave no reliable results because the most relevant part of the LMCT band is masked by the buffer absorption. Reliable results were thus obtained by performing competition experiments, starting from the Pb-saturated peptide and displacing Pb(II) by another cation. Figure 7 shows the results of typical titrations of P^C saturated with Pb(II), with another cation, Zn(II), or Cd(II). These data are correctly fitted with eqs 1 and 2 as demonstrated by the superposition of experimental points with fitted data. In each case, the introduction of the second species $M(P)_2$ was necessary to obtain a good fit. The stability constants are collected in Table 3 and show that Cd(II) is more tightly bound to the CxxC motif than Pb(II), whereas Zn(II) is less tightly bound. Similar competition experiments were conducted with Hg(II), but they could not be correctly fitted because of the very high affinity of this cation for thiolates.[67]

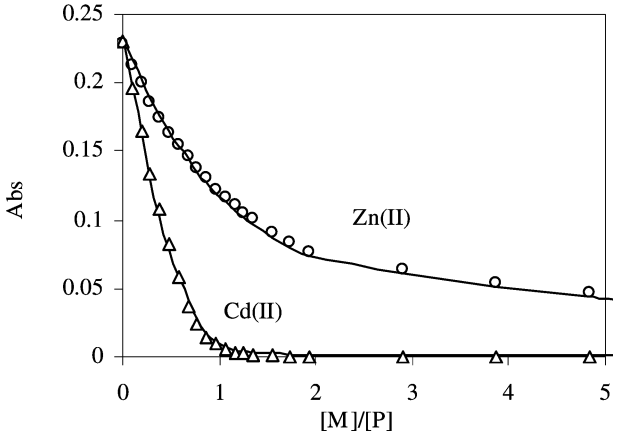

Figure 7. Back-titration of PbP^C ($[P^C] = 71\ \mu M$; $[Pb] = 334\ \mu M$) with $CdCl_2$ (△) and $ZnCl_2$ (○) at pH 7 (20 mM Bis-Tris). Comparison of calculated absorbance (line) and observed absorbance (△, ○) at 315 nm. Calculated lines have been generated in SPECFIT, with the stability constants of Pb(II), Cd(II), and Zn(II) complexes reported in Table 3.

Data collected in Table 3 show that the affinity constants obtained with the cyclic peptide P^C are systematically higher than those measured with its linear analogue P^L. This effect is also evidenced with Hg(II) adducts. Indeed, even if stability constants for this cation are not directly accessible, it was possible to get a rough estimate of the difference in affinities between the two peptides by NMR. The ^{1}H NMR spectrum of an equimolar sample of P^C, P^L, and $HgCl_2$ only shows the lines of the complex HgP^C and the apopeptide P^L. This leads to at least 2 orders of magnitude enhancement in affinity for the Hg complex of the cyclic peptide P^C.

Previously reported stability constants with P^C were deduced from NMR titrations and were rough estimates because the formation of the MP_2 complexes was not taken into account.[39] Nevertheless, these preliminary results indicated a selectivity for Hg(II) and Cu(I) over Cd(II), Pb(II), and Zn(II) with at least 5 orders of magnitude between these two groups of metal ions. This trend is confirmed by the stability constants calculated accurately from UV titration data (Table 3), indicating that the selectivity is even better: 7 orders of magnitude between Cu(I) and Cd(II) and 10 between Cu(I) and Zn(II).

Cu(I) Binding. It has been demonstrated that the metallochaperone Atx1 binds Cu in its I+ oxidation state via the two S atoms of the cysteines of the binding loop of the protein. Binding of Cu(I) with the two model peptides P^C and P^L was thus investigated in a way similar to that of the divalent metal cations. It is known that Cu(I) disproportionates in Cu(0) and Cu(II) in water. Therefore, the experiments with this cation were conducted in the presence of acetonitrile, which associates with Cu(I) and overcomes the disproportionation reaction.[68] Binding of Cu(I) to the peptides was monitored by UV spectroscopy. The addition of aliquots

(66) Magyar, J. S.; Godwin, H. A. *Anal. Biochem.* **2003**, *320*, 39−54.

(67) Wright, J. G.; Natan, M. J.; MacDonnel, F. M.; Ralston, D.; O'Halloran, T. V. In *Progress in Inorganic Chemistry*; Lippard, S. J., Ed.; Wiley: New York, 1990; Vol. 38, pp 323−412.

(68) Kamau, P.; Jordan, R. B. *Inorg. Chem.* **2001**, *40*, 3879−3883.

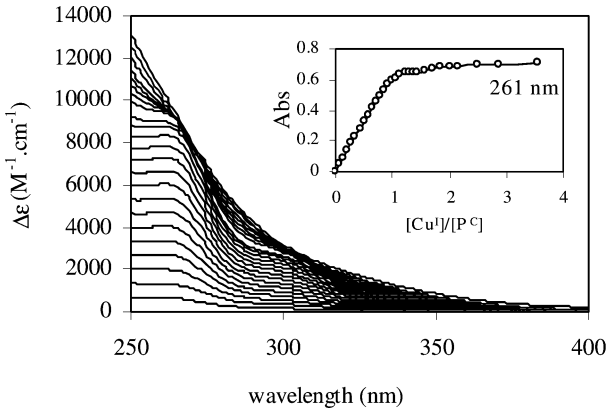

Figure 8. UV titration of P^C (70 μM) with Cu at pH 7 [20 mM Bis-Tris/acetonitrile, 50:50 (v/v)]. Spectra shown are difference spectra [$\Delta\epsilon = \epsilon(CuP^C) - \epsilon(P^C)$] and correspond to samples with 0−3 equiv of Cu(I) per P^C. The inset shows the absorbance at 261 nm vs equiv of Cu(I) per P^C.

of tetrakis(acetonitrile)copper(I) hexafluorophosphate dissolved in acetonitrile over a peptide solution in a 1:1 mixture of Bis-Tris (20 mM, pH 7) and acetonitrile displays the appearance of a single band centered at 261 nm with a sharp end point for 1 equiv. This band is characteristic of thiolate-to-Cu(I) charge-transfer transitions.[69] The same behavior is observed when the titration is conducted in Bis-Tris (20 mM, pH 7) alone or in the presence of TCEP. In excess of Cu(I), another transition appears that is partially obscured by the buffer and that may be attributed to the formation of often-encountered copper(I) thiolate clusters.[69,70] The typical absorption spectra of Cu(I) into a solution of P^C at pH 7 are illustrated in Figure 8.

To get information about the molecularity of Cu(I)/peptide complexes, we performed diffusion coefficient measurements because SEC−HPLC experiments could not be conducted without oxidation of Cu(I). Pulsed-gradient spin−echo NMR diffusion measurements have proved to be a useful tool for probing the presence of unimolecular, bimolecular, or oligomeric species in solution.[71,72] Indeed, the diffusion constant D can be related to the hydrodynamic radii of the molecules via the Stokes−Einstein equation (3), where k is

$$D = kT/6\pi\eta r_H \qquad (3)$$

Boltzmann's constant, T the absolute temperature, η the viscosity, and r_H the hydrodynamic radius of the diffusing species, considered as a hypothetical hard sphere that diffuses with the same speed as the particle under examination. The determination of D by diffusional NMR for shape-similar complexes and ligands is thus an efficient tool for deducing the molecular mass of an unknown species (i, molar mass M_i) in solution, when a reference compound (r, molar mass M_r) is measured under the same conditions (eq 4).[73]

$$\frac{D_i}{D_r} = \sqrt[3]{\left\{\frac{M_r}{M_i}\right\}} \qquad (4)$$

To validate the method for our systems, we have first studied the Hg complex of P^C, which has been demonstrated to be a monomeric complex in solution (NMR and SEC−HPLC). The diffusion coefficients of the free peptide P^C and the complex HgP^C were measured in deuterium oxide: $D(P^C) = 2.5(1) \times 10^{-10}$ m^2 s^{-1} and $D(HgP^C) = 2.35(10) \times 10^{-10}$ m^2 s^{-1}. The hydrodynamic radii calculated from eq 3, with η being the viscosity of deuterium oxide (1.1×10^{-3} kg s^{-1} m^{-1}), are respectively 8.0(3) and 8.5(4) Å. Although the peptide species observed here are not spherical, these r_H values are comparable with the distances measured in the NMR structures (Figure 2). The molar mass of the complex deduced from the mass of the free peptide and the diffusion constants is $M(HgP^C) \approx 1200(400)$ g mol^{-1} in accordance with 1180 g mol^{-1} calculated for the monometallic complex $Hg(P^C)$.

The Cu complexes were analyzed in water/acetonitrile mixtures (9:1, v/v) to avoid disproportionation of Cu(I). The diffusion coefficients of the two peptides were $D(P^C) = 2.05(10) \times 10^{-10}$ m^2 s^{-1} and $D(P^L) = 1.9(1) \times 10^{-10}$ m^2 s^{-1}. The D value obtained for the cyclic peptide P^C is smaller than the preceding one in deuterium oxide because the viscosities of water/acetonitrile mixtures at low acetonitrile contents are higher than that of water alone (here $\eta \approx 1.2 \times 10^{-3}$ kg s^{-1} m^{-1}).[74] The hydrodynamic radii calculated with eq 3 are 8.8(4) and 9.1(5) Å for the cyclic and linear peptides, respectively. $D(CuP^C)$ and $D(CuP^L)$ in the same solvent were $2.0(1) \times 10^{-10}$ m^2 s^{-1} and $1.75(10) \times 10^{-10}$ m^2 s^{-1}, respectively. Application of eq 4 leads to $M(CuP^C) \approx 1100(300)$ g mol^{-1} and $M(CuP^L) \approx 1300(500)$ g mol^{-1}, which compares reasonably well with 1041 and 1110 g mol^{-1} calculated for the monometallic Cu complexes P^C and P^L.

This set of data shows that a monomeric complex Cu(P) is formed as for the protein Atx1.[13,14] In our case, the coordination sphere is probably completed by acetonitrile or buffer molecules because no reducing agent is present in the solution.

To determine the affinity constants of the two Cu(I)/peptide complexes (CuP), we performed UV−visible titrations in the presence of a chelator of known affinity. Bathocuproine disulfonate (Na_2bcs) has been demonstrated to form a stable 1:2 complex, $Cu(bcs)_2^{3-}$, according to eq 5 with a constant $\log \beta_{12} = 19.8$.[70]

$$Cu^+ + 2bcs^{2-} = Cu(bcs)_2^{3-} \qquad (5)$$

The complex $Cu(bcs)_2^{3-}$ exhibits an absorption band in the visible region with an absorption maximum at 483 nm ($\epsilon = 13\,300$ M^{-1} cm^{-1}). Titration of the peptides P^C and P^L

(69) Fujisawa, K.; Imai, S.; Kitajima, N.; Moro-oka, Y. *Inorg. Chem.* **1998**, *37*, 168−169.
(70) Xiao, Z.; Loughlin, F.; George, G. N.; Howlett, G. J.; Wedd, A. G. *J. Am. Chem. Soc.* **2004**, *126*, 3081−3090.
(71) Alajarin, M.; Pastor, A.; Orenes, R.-A.; Martinez-Viviente, E.; Pregosin, P. S. *Chem.−Eur. J.* **2006**, *12*, 877−886.
(72) Terazzi, E.; Torelli, S.; Bernardinelli, G.; Rivera, J.-P.; Bénech, J.-M.; Bourgogne, C.; Donnio, B.; Guillon, D.; Imbert, D.; Bünzli, J.-C. G.; Pinto, A.; Jeannerat, D.; Piguet, C. *J. Am. Chem. Soc.* **2005**, *127*, 888−903.
(73) Waldeck, A. R.; Kuchel, P. W.; Lennon, A. J.; Chapman, B. E. *Prog. Nucl. Magn. Reson. Spectrosc.* **1997**, *30*, 39−68.
(74) Vierk, A.-L. *Z. Anorg. Chem.* **1950**, *261*, 283−296.

preloaded with Cu(I) with aliquots of the competitor (bcs^{2-}) solution shows the appearance of the absorption band of $Cu(bcs)_2^{3-}$, which corresponds to the transfer of the metal cation from the peptide to bcs^{2-}. These spectroscopic data could be fitted with the program SPECFIT according to eq 6 and led to similar affinity constants for the two peptides: $\log \beta_{11}(P^C) = 16.6(1)$ and $\log \beta_{11}(P^L) = 16.4(1)$. No mixed-ligand complexes have been detected in those titrations. Experiments performed in the reverse direction of eq 6, starting with the complex $Cu(bcs)_2^{3-}$ and adding a peptide solution, gave the same results.

$$CuP + 2bcs^{2-} = P + Cu(bcs)_2^{3-} \quad (6)$$

The values of the affinity constants determined for the Cu complexes of the peptides are somewhat lower than the one reported by Wedd with the chaperone Atx1 ($\log \beta = 18.3$).[70]

Discussion

The amino acid sequence MxCxxC appears in many transporters involved in cellular metal trafficking, like copper metallochaperones or ATPases. The selectivity of this sequence for metal ions is thus of fundamental interest in order to understand the mechanisms of metal homeostasis in living organisms. The design of small peptides that mimic the binding loop of these transporters allowed us to focus on the complexation properties of this particular binding site and to measure unambiguously the affinity and selectivity of this motif toward a series of metal cations bound to this sequence in vivo.

The complexation properties of the cyclic and linear decapeptides P^C and P^L are very close: the same metal complexes are obtained with both peptides. The comparison of the complexation behaviors of these two model peptides shows that the introduction of a β turn with the xPGx motif in the cyclic peptide does not disturb the coordination of metal cations. Furthermore, the cyclic peptide gives systematically greater affinity constants than its unstructured linear analogue. This effect (up to 2 orders of magnitude difference for β_{11} constants between HgP^C and HgP^L) can be attributed to the preorganization of the binding loop in the cyclic peptide that predisposes the two cysteine S groups on the same side of the peptidic macrocycle. In comparison, the linear compound has a random-coil conformation and is fully unstructured. The β turn is thus a good way of mimicking the anchor effect of the rest of the protein structure onto the solvent-exposed binding loop.

To get a reliable and absolute stability scale, we first determined the nature of the complexes formed in solution by complementary experimental methods such as MS, SEC, and UV spectroscopy. Affinity measurements were then performed without any reducing agent that would interfere in the complexation reactions. Indeed, such titrations have been often conducted with thiol reducing agents, like dithiothreitol (DTT) or glutathione, to prevent oxidation of the peptide cysteines. However, these agents are also efficient chelators of the metal cations studied here.[67,75] Therefore, the comparison of constants obtained in the presence of reducing agents is not reliable for different metal ions that have variable affinities for the thiol agent. Finally, we selected Bis-Tris as a buffer because its affinities are known with the cations studied here and could thus be taken into account to obtain nonrelative affinity constants that can be compared from one cation to another.

The evolution of the LMCT transitions clearly shows that 1:1 complexes are obtained with Hg(II) and Cu(I), whereas 1:2 and 1:1 (M/P) species are successively formed with Pb(II) and Cd(II). As suggested by ESMS experiments and further demonstrated by SEC or diffusion coefficient measurements, no oligomeric complexes corresponding to M_xP_x cluster-type species are formed. Even though the absolute constant could not be measured for Hg, which is too tightly bound, NMR experiments show that Hg(II) fully displaces Cu(I) in the peptide complex. This leads to a difference of at least 2 orders of magnitude in β_{11}: $\log \beta_{11}(Hg) - \log \beta_{11}(Cu) \geq 2$. The affinity constants ($\log \beta_{11}$) range in the order Hg(II) > Cu(I) ≫ Cd(II) > Pb(II) > Zn(II).

The relative order of the binding affinities found with the two model peptides P^C and P^L and the series of metal ions studied in this paper correlates well with published data obtained with S ligands such as DTT[75] or S-rich proteins such as metallothioneins.[76,77] The neutral S atom of methionine does not participate in the coordination of the metal ions. Indeed, the methionine methyl protons in the NMR spectra are not sensitive to the addition of metal ions (their chemical shift remains constant at 2 ppm). As proposed recently in a molecular dynamics study,[78] the role of the methionine-conserved residue would rather be to stabilize the hydrophobic core of the metallochaperones and the internal structure of the metal-binding site, leading to a perfect positioning of the cysteine side chains for metal binding.

It appears that the CxxC motif is not suitable for binding of the Cu(II) ion. Indeed, the thiol groups present in the peptide are oxidized by Cu(II), as has been described previously for glutathione[79] or DTT.[75] By the addition of copper(II) sulfate, the peptides are oxidized into the corresponding disulfide compounds P^{SS} with concomitant reduction of Cu(II) into Cu(I) according to eq 7.

$$P + 2Cu^{2+} = P^{SS} + 2Cu^{+} + 2H^{+} \quad (7)$$

The model peptides P^C and P^L give Cu(I) complexes that are similar to the Cu-loaded protein Atx1. Indeed, monomeric complexes CuP are formed with two thiolates coordinated to the cation. The stabilities of the model complexes are slightly lower than the stability reported for the Cu adduct

(75) Krezel, A.; Lesniak, W.; Jerowska-Bojczuk, M.; Mlynarz, P.; Brasun, J.; Kozlowski, H.; Bal, W. *J. Inorg. Biochem.* **2001**, *84*, 77−88.
(76) Stillman, M. J. *Coord. Chem. Rev.* **1995**, *144*, 461−511.
(77) Nielson, K. B.; Atkin, C. L.; Winge, D. R. *J. Biol. Chem.* **1985**, *260*, 5342−5350.
(78) Poger, D.; Fuchs, J.-F.; Nedev, H.; Ferrand, M.; Crouzy, S. *FEBS Lett.* **2005**, *579*, 5287−5292.
(79) Ciriolo, M. R.; Desideri, A.; Paci, M.; Rotilio, G. *J. Biol. Chem.* **1990**, *265*, 11030−11034.

of the whole protein Atx1.[70] This may indicate another contribution in this latter case, for instance, the presence of exogenous ligands such as glutathione or an extra stabilization due to the structure of the whole protein in comparison to the short amino acid sequence used in the synthetic peptides.

It can be pointed out that our values are much higher than those reported by Opella and co-workers with MerP and an 18-residue linear peptide derived from merP. However, for these latter systems, the affinity measurements have been performed in a large excess of DTT, which dramatically competes with the peptides.[67] Therefore, the apparent binding constants measured are very low ($\log \beta_{11} \approx 4$), and no selectivity could be evidenced from these data.[31]

The interaction of various metal ions with the N-terminal domain of ZntA ATPase (N1−ZntA) has been investigated by Mitra and co-workers.[80] The values of the binding constants determined with Pb(II), Cd(II), and Zn(II) are similar to ours, but this protein contains a second potential binding site (CCCDGAC) in addition to the consensus sequence (MxCxxC). It is therefore difficult to assign these affinities to a precise metal−S interaction. Besides, the authors have demonstrated that certain ions bind to the first site whereas others like Pb(II) and Hg(II) need the presence of the second site sequence to be bound. This exemplifies the necessity of studying model systems that contain only one binding site and comparing them to the whole protein to understand the coordination properties of those multisite proteins.

In conclusion, we have demonstrated that the consensus sequence MxCxxC found in many metal transporters binds Hg(II), Cu(I), Pb(II), Cd(II), and Zn(II) but not Cu(II), which oxidizes the peptides into disulfide compounds. The selectivity, Hg(II) > Cu(I) ≫ Cd(II) > Pb(II) > Zn(II), is in accordance with what is observed with S-rich ligands such as DTT or metallothioneins. This motif is actually very selective for Cu(I), compared to the essential ion Zn(II) that could compete in vivo or compared to the toxic ions Pb(II) and Cd(II). Indeed, these three latter divalent cations have greater affinities for coordination sites having more than two cysteines, like, for instance, Zn finger sites,[38] than for the simple CxxC sequence. Their preference for three or four S environments is also exemplified by the formation of 1:2 (M/P) complexes in excess of peptides, whereas such complexes are not obtained with Cu(I). On the other hand, Hg, which has a very high affinity for S ligands especially in linear bis(thiolate) complexes, may be an efficient competitor in vivo. This approach, using synthetic peptides in vitro, allows us to focus on the metal complexes of a specific binding sequence and to determine its coordination properties and selectivity. It will be applied to other sequences known to play a role in metal homeostasis in order to get a reliable description of the thermodynamic properties of metal cations−amino acid consensus sequence interactions.

Acknowledgment. We thank the program of nuclear toxicology of the Commissariat a l'Energie Atomique for financial support and for the post-doctoral fellowship of O.S. and P.R.-P., the Centre Grenoblois de Résonance Magnétique (CGRM) for use of the Avance 500 NMR spectrometer, Pierre-Alain Bayle for his help in running the NMR experiments, Roger Miras for his help in performing the SEC-HPLC measurements, and Dr. Elisabeth Mintz for very fruitful discussion.

Supporting Information Available: NMR data for P^L and $P^C{}_{SS}$, SEC−HPLC calibration curve, and UV titrations with P^L. This material is available free of charge via the Internet at http://pubs.acs.org.

IC060430B

(80) Liu, J.; Stemmler, A. J.; Fatima, J.; Mitra, B. *Biochemistry* **2005**, *44*, 5159−5167.